IL NUOVO CIMENTO **40 C** (2017) 159
DOI 10.1393/ncc/i2017-17159-5

COLLOQUIA: LaThuile 2017

Galactic center gamma-ray excess and the *Fermi* bubbles

D. MALYSHEV

Erlangen Centre for Astroparticle Physics - Erwin-Rommel-Str. 1, D-91058 Erlangen, Germany

received 16 September 2017

Summary. — The Galactic center (GC) is expected to be the brightest source of possible dark matter (DM) annihilation signal. Excess gamma-ray emission has been detected by several groups. Both DM and more conventional astrophysical explanations of the excess have been proposed. In this report, we discuss possible effects of modeling the *Fermi* bubbles at low latitudes on the GC excess. We consider a template of the *Fermi* bubbles at low latitudes derived by assuming that the spectrum between 1 GeV and 10 GeV at low latitudes is the same as at high latitudes. We argue that the presence of the *Fermi* bubbles near the GC may have a significant influence on the spectrum of the GC excess, especially at energies above 10 GeV.

1. – Introduction

The Galactic center (GC) is expected to be the brightest source of possible annihilation of dark matter (DM) particles [1]. Hints of the excess in the GC were claimed soon after the *Fermi* LAT data became available [2, 3]. It was also argued that the excess has an extension larger than the *Fermi* LAT point spread function [4]. Further studies by several groups have confirmed that the excess is indeed extended with a spectrum peaking around a few GeV [5-8].

Apart from DM annihilation, possible interpretations of the excess include additional sources of cosmic rays (CR) near the GC [9-11], an unresolved population of millisecond pulsars (MSPs) [12-17], *Fermi* bubbles near the Galactic plane (GP) [18, 19]. The interpretation of the GC excess depends crucially on uncertainties related to modeling of the Galactic foreground emission and resolved point sources [20-22].

One of the largest uncertainties in the GC excess is the behavior of the *Fermi* bubbles near the GP [22]. Although the *Fermi* bubbles are relatively easy to model at high latitudes above and below the GP [23, 24], the study the *Fermi* bubbles near the GP suffers from the same uncertainties in the Galactic foreground modeling as the GC excess itself. The problem is further complicated by the absence of a clear counterpart of the *Fermi* bubbles in other frequencies. Numerical modeling of the bubbles [25-28] and observations of lobes in other galaxies show that the bubbles can be either completely

expelled from the GC by the pressure of the gas, or they can have an hourglass shape centered at the GC, or they can have an extended base in the GC. Although the gamma-ray spectrum of the *Fermi* bubbles may change as a function of the latitude due to energy losses, energy dependent propagation effects, or re-acceleration inside the volume of the bubbles, observations suggest that the spectrum of the bubbles is uniform at high latitudes [6, 24].

In this report, we consider a model of the *Fermi* bubbles at low latitudes derived with the assumption that their spectrum is the same at low latitudes as at high latitudes and discuss the effect of including the low latitude bubbles template on the GC excess spectrum. The discussion is based on the results reported in [22].

2. – GC excess with high latitudes bubbles template

In order to study the effect of the *Fermi* bubbles on the GC excess, we first review a derivation of the excess in a model that includes a template for the bubbles at latitudes $|b| > 10^\circ$ [24]. The analysis is based on 6.5 years of *Fermi* LAT data between August 4, 2008 and January 31, 2015, Pass 8 UltraCleanVeto class events with a zenith angle cut $\theta < 90^\circ$. We take the data between 100 MeV and 1 TeV in 27 logarithmic energy bins. The maps are constructed using HEALPix [29] with a pixel size of $\approx 0^\circ.46$ at low latitudes and $\approx 0^\circ.92$ at high latitudes [22].

The model is derived by fitting templates corresponding to different emission components to the data in each energy bin. The templates consist of π^0 and bremsstrahlung emission components separated in five Galactocentric rings derived with GALPROP code [30-33]. The inverse Compton templates are also derived with the GALPROP code. They are separated in three components related to the three interstellar radiation fields (cosmic microwave background, starlight, and infrared components). The other components are Loop I, flat *Fermi* bubbles template at high latitudes, Sun and Moon templates, point sources template (derived with fluxes from the 3FGL catalog). The Large Magellanic cloud, the Cygnus region, and the other extended sources in the 3FGL catalog are treated as independent components. The cores of 200 brightest PS from the 3FGL catalog are masked within 1°. The GC excess is modeled by DM annihilation in generalized NFW profile [34] with index $\gamma = 1.25$, $\rho(r) \propto \frac{1}{r^\gamma (1+r)^{3-\gamma}}$. The spectra of the different components obtained by fitting the templates to the data in each energy bin and the residual with the GC excess emission added back are shown in fig. 1. Although the excess flux integrated over the whole sky is relatively small, $\lesssim 1\%$, the intensity of excess emission near the GC is about 15% of the total gamma-ray intensity in that region.

3. – *Fermi* bubbles template at low latitudes

Since there are no clear counterparts of the *Fermi* bubbles in other frequencies that can be used to derive a template of the gamma-ray emission, one needs to make some assumption to construct a model of the bubbles at low latitudes. The assumption that we will make is that the spectrum of the bubbles at low latitudes is the same as at high latitudes in the energy range between 1 GeV and 10 GeV.

In order to derive the bubbles template, we first model the gamma-ray emission by the gas-correlated templates (π^0 and bremsstrahlung), PS, and a combination of smooth components, which are introduced to provide a generic model for the other components of emission, such as the Loop I and the bubbles. Then we subtract the gas-correlated components and the point sources from the data and decompose the remaining residuals

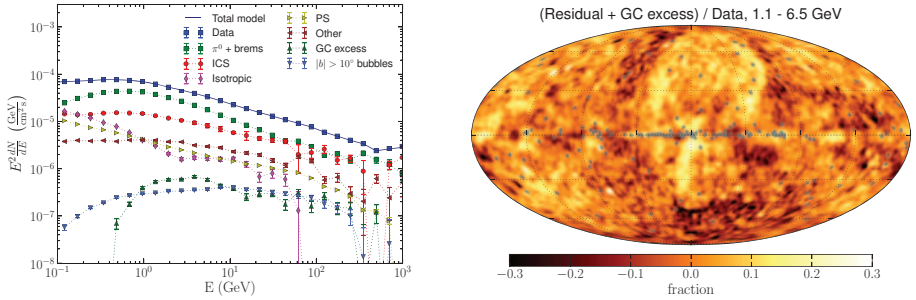

Fig. 1. – Left: spectrum of components of gamma-ray emission in a model with *Fermi* bubbles determined at $|b| > 10^\circ$. "Other" components include Loop I, extended sources, Sun, and Moon templates. See sect. **2** for more details on the different components of emission. Right: fractional residual in the model with spectra shown on the left plot summed over energy bins between 1.1 GeV and 6.5 GeV plus the GC excess modeled by the gNFW DM annihilation template.

between 1 GeV and 10 GeV into two components correlated with $\propto E^{-1.9}$ and $\propto E^{-2.4}$ spectra. The former spectrum is the spectrum of the *Fermi* bubbles at high latitudes, the latter one is the average spectrum of the other astrophysical components: Loop I, IC, and isotropic. The residual after subtracting the gas-correlated emission and PS from the data and the two spectral components are shown in fig. 2. Then we introduce a cut in significance at 2σ level of the $\propto E^{-1.9}$ component to derive the *Fermi* bubbles template (fig. 3).

An alternative template of the bubbles as well as a template of the GC excess can be derived if we separate the residuals after subtracting the gas-correlated components and PS from the data into three spectral components, where the first two components have the same spectra as before ($\propto E^{-1.9}$ and $\propto E^{-2.4}$) while for the third component we take an average spectrum of MSPs $\propto E^{-1.6}e^{-E/4\,\mathrm{GeV}}$ [35, 36]. The maps for the bubble-like and MSP-like spectral components are shown in fig. 4.

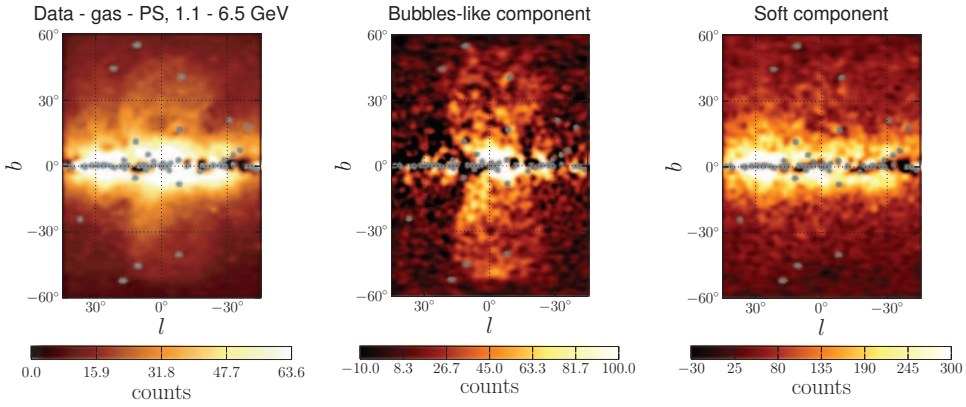

Fig. 2. – Left panel: residual obtained by subtracting gas-correlated components of emission (π^0 and bremsstrahlung) and PS from the data. These residuals are decomposed into two spectral components: $\propto E^{-1.9}$ spectrum (middle panel) and $\propto E^{-2.4}$ spectrum (right panel).

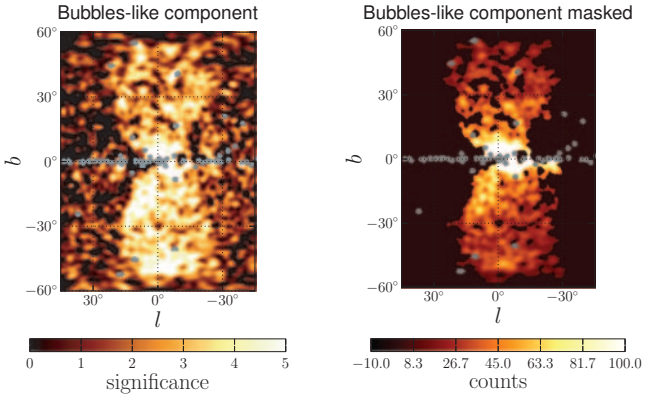

Fig. 3. – Left: significance map of the $E^{-1.9}$ spectral component in the middle panel of fig. 2. Right: bubbles template obtained from the $E^{-1.9}$ spectral component by cutting at 2σ significance in the left plot and taking the connected component.

The effect of including the all-sky bubbles template on the GC excess flux is shown in fig. 5. We see that the GC excess flux is completely absorbed by the *Fermi* bubbles template at $E > 10\,\mathrm{GeV}$ and it is reduced by a factor $\gtrsim 2$ below $10\,\mathrm{GeV}$.

4. – GC excess and *Fermi* bubbles near the GC

In this section we briefly discuss the morphology of the bubble-like and the MSP-like spectral components. The latitude profile plots for the spectral components maps in fig. 4 are shown in fig. 6.

The bubble-like component is shown on the left. The distribution is flat at latitudes $10^\circ < |b| < 50^\circ$. The flatness of the profile is especially clear at negative latitudes where there is less overlap with the local gas clouds compared to positive latitudes. However, close to the GP, there is an increase in the intensity of emission for longitudes $\ell = 0^\circ$, -5° by a factor 3 to 4 compared to high latitudes, while the intensity around $\ell = 5^\circ$ is consistent with zero. Thus, the intensity of emission from the *Fermi* bubbles appears to

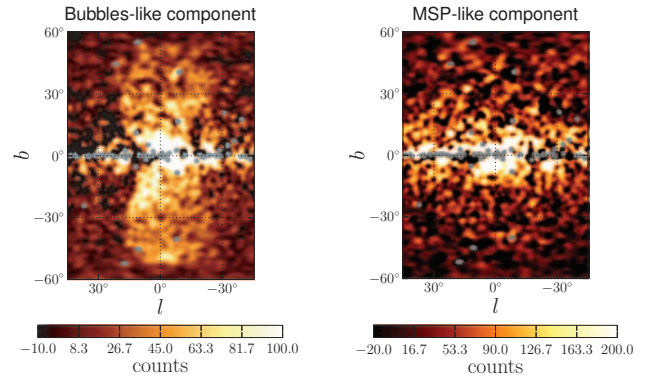

Fig. 4. – Bubble-like $\propto E^{-1.9}$ (left panel) and MSP-like $\propto E^{-1.6}e^{-E/4\,\mathrm{GeV}}$ (right panel) spectral components obtained in three-component decomposition of the residuals in the left panel of fig. 2.

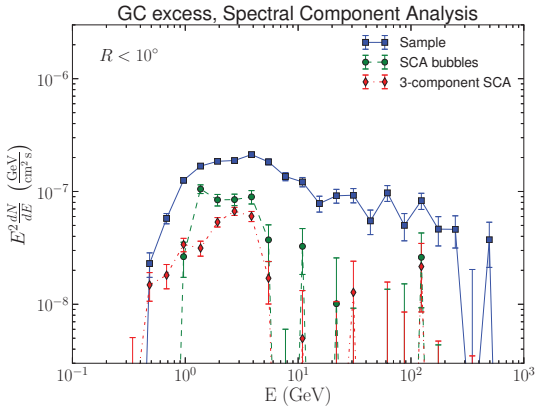

Fig. 5. – Spectrum of the excess integrated within 10° from the GC. The "Sample" model corresponds to the GC excess spectrum in fig. 1 on the left. It is derived with the *Fermi* bubbles template for $|b| > 10^\circ$. In the "SCA bubbles", the bubbles template is presented in fig. 3 on the right, while the GC excess is modeled by the gNFW template. In the "3-component SCA" model with bubbles and the GC excess templates are derived from the "Bubbles-like" and "MSP-like" spectral components in fig. 4, respectively.

have larger intensity near the GP for longitudes $\ell \lesssim 0^\circ$. The apparent asymmetry of the *Fermi* bubbles with respect to the GC may have implications for the interpretation of the *Fermi* bubbles as emanating from the supermassive black hole at the GC. The presence of the asymmetry is subject to large uncertainties in the distribution of gas towards the GC [22] and needs to be investigated further.

The latitude profiles for the MSP-like spectral component exhibit a morphology consistent with spherical symmetry with respect to the GC. There is a slight excess of emission in the GP at $\ell = \pm 5^\circ$, $b = 0^\circ$ relative to the off plane locations $b = \pm 5^\circ$, $\ell = 0^\circ$. If this component is indeed coming from MSPs, then the slightly higher intensity along the GP can be interpreted as contribution of MSPs in the disk of the Galaxy on top of the MSPs in the bulge. One can also see the slightly larger emission along the GP in fig. 4 on the right. Overall, we find that the spectral component derived with MSP-like spectrum is generally consistent with the expectations for the distribution of MSPs in the Galaxy.

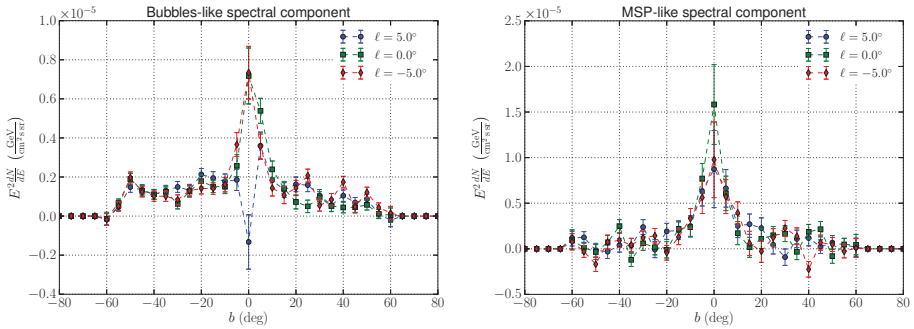

Fig. 6. – Latitude profiles of the bubble-like (left) and MSP-like (right) spectral components in fig. 4. The normalization corresponds to the intensity of these components at 2 GeV.

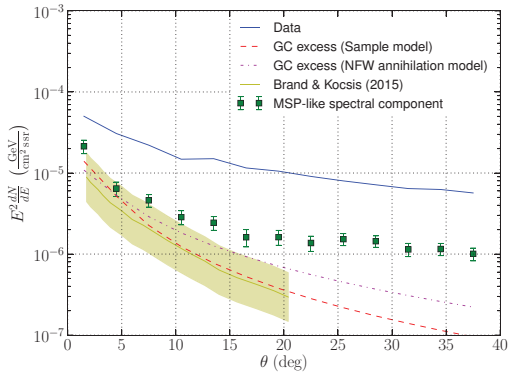

Fig. 7. – Radial profile of the MSP-like spectral component in fig. 4 on the right.

The radial profile of the MSP-like component is shown in fig. 7. Within $\approx 7^\circ$ the profile is consistent with the GC excess modeled by the gNFW profile (sect. **2**). The deviation at large distances from the GC can be interpreted as the contribution of the MSPs in the GP.

5. – Conclusions

In this report we discuss a derivation of the *Fermi* bubbles template at low latitudes and the effect of the inclusion of this template in the model for Galactic emission on the spectrum of the GC excess. We find that the *Fermi* bubbles near the GP may have an intensity 3 to 4 times higher than at high latitudes. The bubbles in the GP may also have asymmetric distribution with respect to the GC: in our model, the intensity of the *Fermi* bubbles at positive latitudes is significantly smaller than the intensity at negative latitudes. We also find that modeling of the *Fermi* bubbles near the GP can have a significant impact on the properties of the GC excess. In the presence of the all-sky bubbles template, the GC excess flux is consistent with zero above 10 GeV and is reduced by a factor of about 2 or more below 10 GeV compared to the model with the bubbles template determined for $|b| > 10^\circ$.

Future observations, such as the Cherenkov Telescope Array may be able to detect the higher intensity emission from the *Fermi* bubbles in the GP. If the spectrum of the *Fermi* bubbles in the GP does not have a softening or a cutoff observed at high latitudes [24], then it may be possible to detect neutrino emission from the *Fermi* bubbles with IceCube and KM3NeT in the hadronic model of gamma-ray emission. Further study of the microwave counterpart of the *Fermi* bubbles at low latitudes may help to discriminate the leptonic and hadronic models of the gamma-ray emission. Progress in understanding of the *Fermi* bubbles near the GC will help to get a more precise description of the GC excess, which will help to disentangle its nature.

* * *

The *Fermi* LAT Collaboration acknowledges support from NASA and DOE (United States), CEA/Irfu, IN2P3/CNRS, and CNES (France), ASI, INFN, and INAF (Italy), MEXT, KEK, and JAXA (Japan), and the K. A. Wallenberg Foundation, the Swedish Research Council, and the National Space Board (Sweden). This work was partially supported by NASA grants NNX14AQ37G and NNH13ZDA001N.

REFERENCES

[1] Kuhlen M., Madau P. and Silk J., *Science*, **325** (2009) 970.
[2] Goodenough L. and Hooper D., arXiv:0910.2998 (2009).
[3] Vitale V. and Morselli A. for the Fermi LAT Collaboration, arXiv:0912.3828 (2009).
[4] Hooper D. and Linden T., *Phys. Rev. D*, **84** (2011) 123005.
[5] Abazajian K. N. and Kaplinghat M., *Phys. Rev. D*, **86** (2012) 083511.
[6] Hooper D. and Slatyer T. R., *Phys. Dark Univ.*, **2** (2013) 118.
[7] Gordon C. and Macías O., *Phys. Rev. D*, **88** (2013) 083521.
[8] Daylan T., Finkbeiner D. P., Hooper D., Linden T., Portillo S. K. N., Rodd N. L. and Slatyer T. R., *Phys. Dark Univ.*, **12** (2016) 1.
[9] Cholis I., Evoli C., Calore F., Linden T., Weniger C. and Hooper D., *J. Cosmol. Astropart Phys.*, **12** (2015) 005.
[10] Gaggero D., Taoso M., Urbano A., Valli M. and Ullio P., *J. Cosmol. Astropart Phys.*, **12** (2015) 056.
[11] Carlson E., Linden T. and Profumo S., *Phys. Rev. Lett.*, **117** (2016) 111101.
[12] Grégoire T. and Knödlseder J., *Astron. Astrophys.*, **554** (2013) A62.
[13] Yuan Q. and Zhang B., *J. High Energy Astrophys.*, **3** (2014) 1.
[14] Petrović J., Serpico P. D. and Zaharijas G., *J. Cosmol. Astropart Phys.*, **2** (2015) 023.
[15] Bartels R., Krishnamurthy S. and Weniger C., *Phys. Rev. Lett.*, **116** (2016) 051102.
[16] Lee S. K., Lisanti M., Safdi B. R., Slatyer T. R. and Xue W., *Phys. Rev. Lett.*, **116** (2016) 051103.
[17] Brandt T. D. and Kocsis B., *Astrophys. J.*, **812** (2015) 15.
[18] Yang R.-Z. and Aharonian F., *Astron. Astrophys.*, **589** (2016) A117.
[19] Macias O., Gordon C., Crocker R. M. *et al.*, arXiv:1611.06644 (2016).
[20] Calore F., Cholis I. and Weniger C., *J. Cosmol. Astropart Phys.*, **3** (2015) 038.
[21] Ajello M., Albert A., Atwood W. B. *et al.*, *Astrophys. J.*, **819** (2016) 44.
[22] The Fermi LAT Collaboration, arXiv:1704.03910 (2017).
[23] Su M., Slatyer T. R. and Finkbeiner D. P., *Astrophys. J.*, **724** (2010) 1044.
[24] Ackermann M., Albert A., Atwood W. B. *et al.*, *Astrophys. J.*, **793** (2014) 64.
[25] Zubovas K. and Nayakshin S., *Mom. Not. R. Astron. Soc.*, **424** (2012) 666.
[26] Guo F., Mathews W. G., Dobler G. and Oh S. P., *Astrophys. J.*, **756** (2012) 182.
[27] Yang H.-Y. K., Ruszkowski M., Ricker P. M., Zweibel E. and Lee D., *Astrophys. J.*, **761** (2012) 185.
[28] Mou G., Yuan F., Bu D., Sun M. and Su M., *Astrophys. J.*, **790** (2014) 109.
[29] Górski K. M., Hivon E., Banday A. J., Wandelt B. D., Hansen F. K., Reinecke M. and Bartelmann M., *Astrophys. J.*, **622** (2005) 759.
[30] Strong A. W., Moskalenko I. V. and Reimer O. *Astrophys. J.*, **613** (2004) 962.
[31] Ptuskin V., Moskalenko I. V., Jones F. *et al.*, *Astrophys. J.*, **642** (2006) 902.
[32] Porter T. A., Moskalenko I. V., Strong A. W. *et al.*, *Astrophys. J.*, **682** (2008) 400.
[33] Vladimirov A. E., Digel S. W., Johannesson G. *et al.*, *Comput. Phys. Commun.*, **182** (2011) 1156.
[34] Zhao H., *Mom. Not. R. Astron. Soc.*, **278** (1996) 488.
[35] Cholis I., Hooper D. and Linden T., arXiv:1407.5583 (2014).
[36] McCann A., *Astrophys. J.*, **804** (2015) 86.